The effect of calcination temperature and atmosphere on the photocatalytic properties of g-C₃N₄

J. M. Zhao, R. Wang, L. L. Wang, T. Wang, Y. P. Pan, X.H. Shui, Y. Sun* School of Mechanical Engineering, Chengdu University, Chengdu, 610106, China

This study focused on the synthesis of g-C₃N₄ derived from three distinct precursors (dicyandiamide, melamine, urea). The synthesis was conducted through a thermal polymerization method under varying atmospheric conditions (air and nitrogen). The photocatalytic performance was assessed based on the assessment of the degradation rate of tetracycline, and the results revealed that g-C₃N₄ prepared at a calcination temperature of 550°C under nitrogen atmosphere exhibited the highest degradation rate of 59.9% within 60 min, using urea as precursor. Further analysis indicated that g-C₃N₄ synthesized via thermal polymerization under nitrogen atmosphere demonstrated a larger specific surface area, which could increase the active sites and enhance the photocatalytic activity.

(Received July 2, 2025; Accepted October 13, 2025)

Keywords: Thermal polymerization, g-C₃N₄, Photocatalytic degradation, Tetracycline

1. Introduction

Tetracycline (TC), a type of antibiotic, has been extensively applied in the medical domain. Nevertheless, some microorganisms in certain water bodies and soil are nearly extinct due to the misuse of tetracycline, which also results in the development of resistance and mutation in various bacteria. Additionally, the misuse of tetracycline could aggravate the risk of human diseases, posing a significant threat to human life and health [1-3]. Therefore, it is in urgent need to seek an efficient and appropriate approach to address this issue. Generally, the methods for TC degradation are composed of the adsorption method [4], biodegradation method [5], and electrochemical oxidation method [6]. However, these conventional methods tend to be restricted by low efficiency. With the development of technologies, photocatalysis has gained widespread attention based on the advantages of cleanliness, environmental friendliness, ease of operation, and low cost [7,8]. Functionally, light energy could be utilized in photocatalysis technology as the driving force for numerous catalysts, which exhibits a unique advantage in treating a wide range of water antibiotic pollution [9].

Graphite carbon nitride $(g-C_3N_4)$ is a typical photocatalyst with a suitable bandgap (~ 2.7 eV), and it has been widely applied due to high chemical stability, non-toxicity, ease of preparation, and [10-12]. Specifically, $g-C_3N_4$ represents a novel class of carbon-nitrogen compounds, in which the graphite-like layer structure and high nitrogen content render it a material with considerable application potential across various fields, including photocatalysis and energy storage [13]. Typically, $g-C_3N_4$ can be prepared through various precursors, such as urea, thiourea, dicyandiamide and melamine [14]. Besides, numerous methods could be employed for the fabrication of $g-C_3N_4$,

^{*}Corresponding author: sunyan@cdu.edu.cn https://doi.org/10.15251/DJNB.2025.204.1275

including high-temperature thermal polymerization, microwave-assisted heating, solvothermal synthesis, and the supramolecular preassembly method [15]. Among these methods, the thermal polymerization method is a facile synthesis of g-C₃N₄ based on condensation polymerization. However, g-C₃N₄ synthesized by the traditional thermal polymerization method exhibits the disadvantages of low specific surface area, low polymerization degree, and low degree of crystallinity, which will result in a serious agglomeration phenomenon. Besides, it could limit the number of active sites and induce the rapid electron-hole recombination, leading to the reduction of charge carrier mobility, ultimately exhibiting a negative effect on its activity as a photocatalyst [16].

To solve the above problems, in this work, g-C₃N₄ was synthesized using three precursors (dicyandiamide, melamine, and urea). The influence of temperature and atmosphere conditions on the structure and photocatalytic properties of the catalyst was comprehensively investigated to explore the optimal preparation parameters of g-C₃N₄ with superior photocatalytic performance.

2. Experimental

2.1. Synthesis of photocatalysts

Thermal polymerization was used for the synthesis of bulk g-C₃N₄ [17]. Firstly, 10 g of dicyandiamide/melamine/urea was accurately weighed and added into a crucible with a lid. Then, the crucible was placed into a tube furnace, and heated at 550 °C for 4 hours under different atmospheres (air, nitrogen). After naturally cooling down, the crucible was removed, and the yellow product was ground into powder. Subsequently, the product was washed with deionized water and dried at 70 °C. The g-C₃N₄ obtained using dicyandiamide, melamine, and urea under air conditions were named DCN-Air, MCN-Air, and UCN-Air, respectively, while those prepared under nitrogen atmosphere were named DCN-N₂, MCN-N₂, and UCN-N₂. Additionally, in order to investigate the impact of temperature, with dicyandiamide as the precursor, g-C₃N₄ samples were prepared 450 °C, 550°C and 650°C under air and N₂, which were denoted as DCN-450Air, DCN-450N₂, DCN-550Air, DCN-550N₂, DCN-650Air, and DCN-650N₂, respectively.

2.2. Characterization

The phase composition and morphology of the samples were characterized by an X-ray diffractometer (DX-2700B) and a scanning electron microscope (SEM, ZEISS Sigma 300), respectively. The structure of functional groups in the catalyst was determined by a Nicolet iS20 Fourier transform infrared (FT-IR) spectrometer, and the specific surface area of the catalyst were tested by a V-Sorb 2800P analyzer.

2.3. Photocatalytic experiment

The photocatalytic performance of the prepared catalysts was assessed according to the degradation of TC. A 500 W xenon lamp was employed as the light source with irradiation intensity of 100 mW/cm² (AM 1.5). Firstly, 40 mg of g-C₃N₄ was weighed and put into 100 mL TC solution (20 mg/L), followed by an ultrasonic treatment for 5 minutes. After that, the suspension was stirred in the dark for 30 minutes to achieve the adsorption-desorption balance. After illumination, 2 mL of suspension was extracted every 10 minutes, followed by filtering through a 0.22 μ m filter membrane.

Where after, the ultraviolet-visible spectrophotometer (Persee TU-1901) was employed to test the absorbance of TC solution.

3. Results and discussion

After heat treatment at 550 °C in an air atmosphere and in a nitrogen atmosphere, the XRD patterns of g-C₃N₄ prepared using different precursors are shown in Fig. 1. The two peaks appeared at 13.1° and 27.3° match well with (100) and (002) crystal planes of g-C₃N₄, respectively (JCPDS 87-1526) [18]. The peak at 13.1° corresponds to the in-plane structural stacking of the triazine unit, while the peak at 27.3° is indexed to the interlayer stacking of aromatics. Notably, it is clear that the intensity of diffraction peaks for DCN-N₂ is higher and shifted to larger angles on the crystal plane (002), which means higher crystallinity and smaller layer spacing of DCN-N₂.

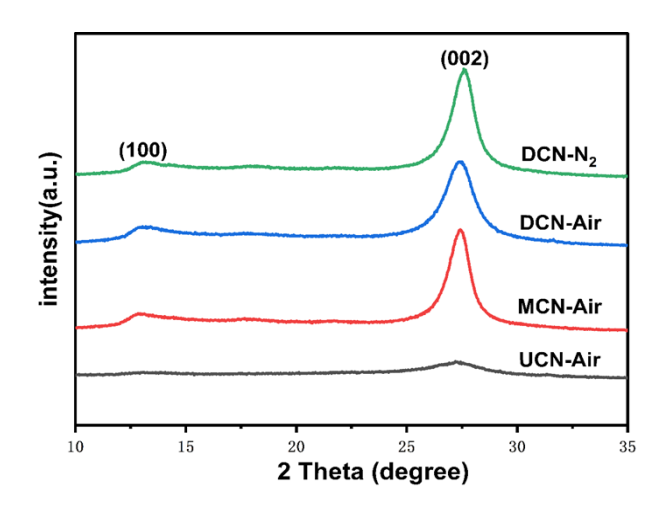


Fig. 1. XRD patterns of DCN-N₂, DCN-Air, MCN-Air and UCN-air.

Fig. 2 depicts the XRD patterns of DCN samples prepared in an air atmosphere and nitrogen atmosphere at varying temperatures. In Fig. 2(a), it could be found that the XRD pattern of sample heated at 450°C in air atmosphere appears to be more heterogeneous, corresponding to the intermediate product composed of C, H, and N elements. Specifically, as the temperature increases, two characteristic diffraction peaks of g-C₃N₄ could be observed in the XRD patterns of DCN-550Air and DCN-650Air samples, without any indication of heterogeneous phases. The similar findings can be seen in Fig. 2(b). Notably, the characteristic diffraction peak of (002) plane exhibits a gradually increasing trend and becomes sharper under nitrogen atmosphere condition at 550°C, which indicates that the layered stacking within the product structure increases with the increased temperature. However, a decreasing trend could be found in intensity for characteristic diffraction peak at 650°C, which could be attributed to the reduced crystallinity caused by the minor breakage of C=N bonds within g-C₃N₄ at higher temperature. Therefore, the application of a thermal treatment temperature of 550°C in a nitrogen atmosphere could produce g-C₃N₄ with higher crystallinity, and g-C₃N₄ could exist stably with good thermal stability performance within this temperature range.

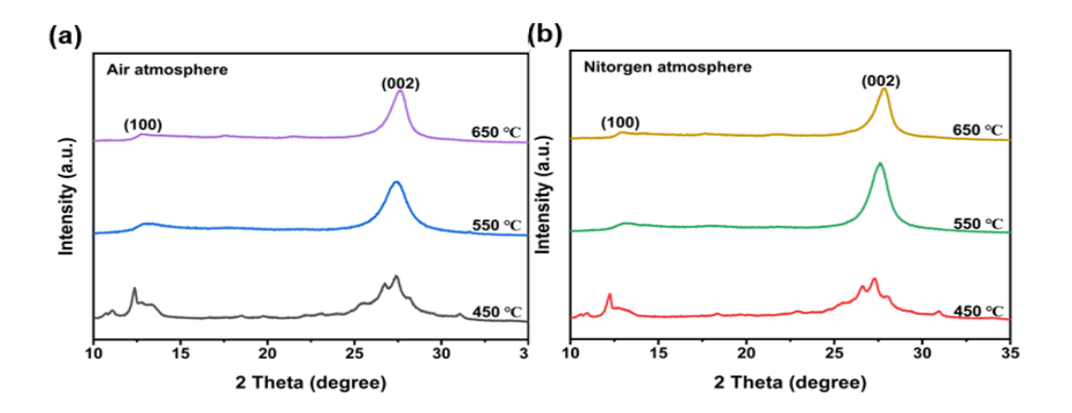


Fig. 2. XRD patterns of DCN samples: (a) under air atmosphere, (b) under nitrogen atmosphere.

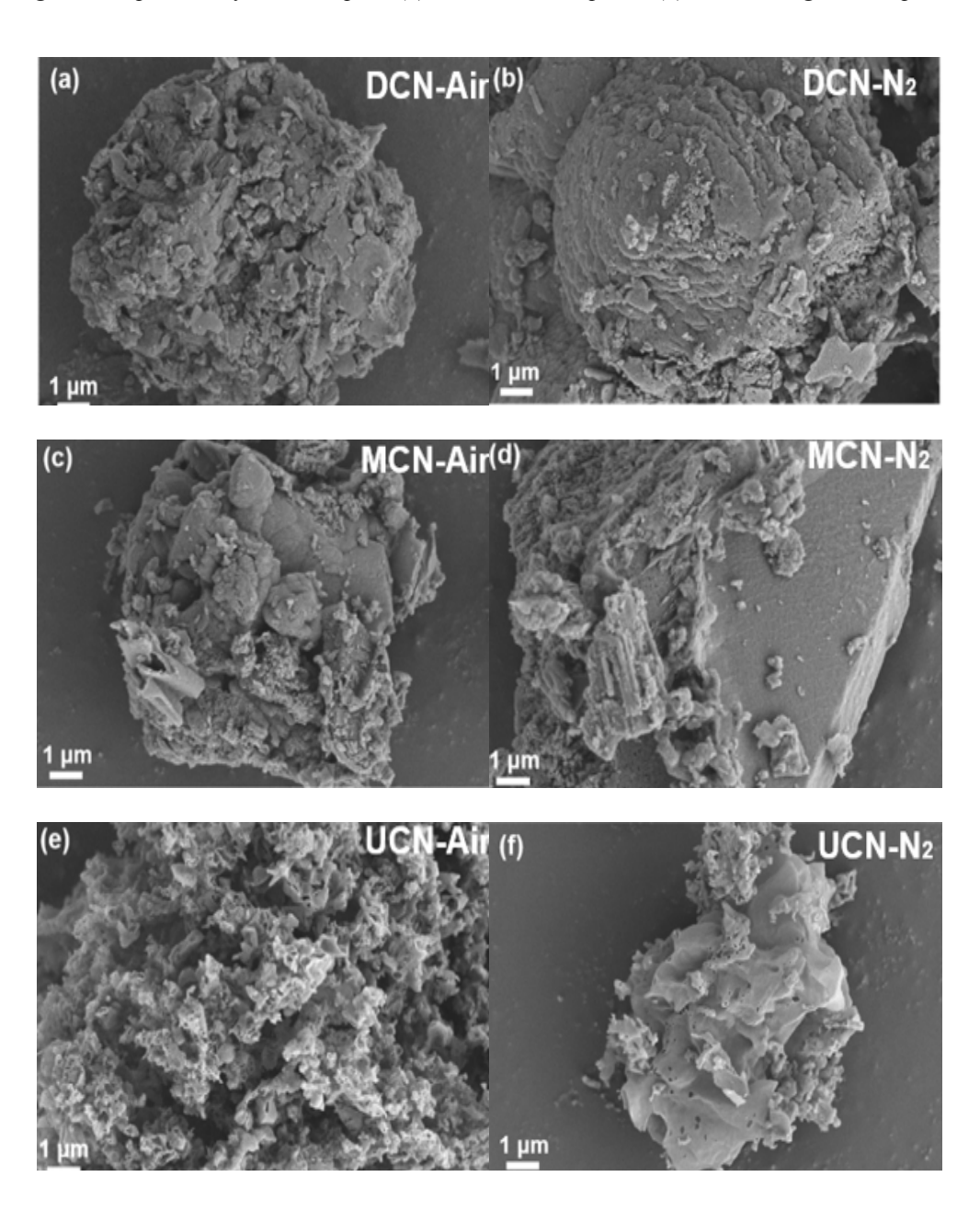


Fig. 3. SEM images of the synthesized samples at 550 °C: (a) DCN-Air, (b) DCN- N_2 , (c) MCN-Air, (d) MCN- N_2 , (e) UCN-Air, (f) UCN- N_2 .

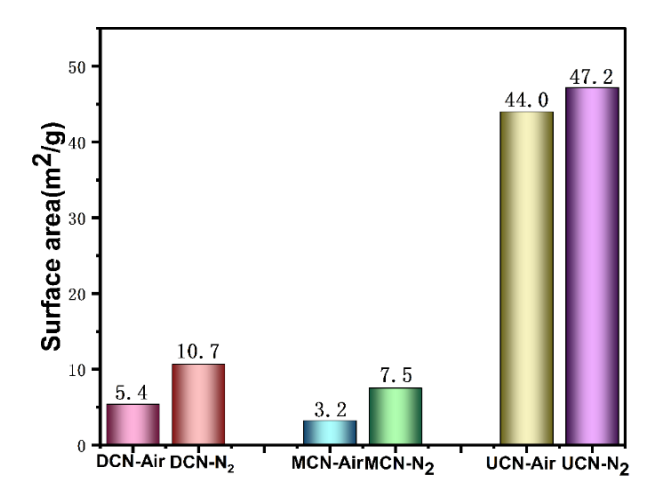


Fig. 4. Specific surface area of DCN, MCN and UCN under air and nitrogen atmospheres.

The surface morphology of g-C₃N₄ derived from three precursors under thermal treatment at 550°C are shown in Fig. 3. According to the results, the three products of DCN-Air, MCN-Air, and UCN-Air exhibit a granular structure with piled-up features and rough surfaces. Conversely, the products prepared under nitrogen atmosphere display smoother surface structures, alongside more obvious laminar features versus those prepared under air atmosphere.

The specific surface areas of the six samples derived from various raw materials under different atmospheres are shown in Fig. 4. According to the results, the specific surface areas of DCN-Air, MCN-Air, and UCN-Air are 5.4, 3.2, and 44.0 m²/g, respectively. Obviously, g-C₃N₄ samples prepared under nitrogen atmosphere exhibit much larger specific surface areas, which are 10.7, 7.5, and 47.2 m²/g, respectively. Notably, owing to the porous structure, the g-C₃N₄ obtained by urea exhibits a larger specific surface area than the products obtained by melamine and dicyandiamide. Therefore, it could be concluded that nitrogen atmosphere could increase the specific surface area of g-C₃N₄, providing more active sites for photocatalytic reaction.

Fig. 5 displays FT-IR spectra of dicyandiamide and g-C₃N₄ produced by thermal treatment at 550 °C under nitrogen and air atmospheres. It is seen that the absorption peak of dicyandiamide in the range of 500-800 cm⁻¹ could be assigned to the stretching vibration of the C-NH₂ bond. Meanwhile, the absorption peak in the range of 1000-1800 cm⁻¹ could be indexed to the vibration of the aromatic C-N skeleton [19]. Furthermore, absorption peaks in the range of 1280-1400 cm⁻¹ and 3000-3800 cm⁻¹ correspond to the stretching vibration of the N-H bond. In comparison with dicyandiamide precursor, an absorption peak at 806 cm⁻¹ could be observed in both DCN-Air and DCN-N₂ samples. Notably, this peak is accompanied by a decrease in intensity within the range of 1200-1400 cm⁻¹, which is due to the stretching vibrations of the triazine ring. Additionally, the complete disappearance of absorption peaks in the range of 1400-1820 cm⁻¹ suggests the significant breakdown of nitrogen-hydrogen bonds during the thermal polycondensation reaction.

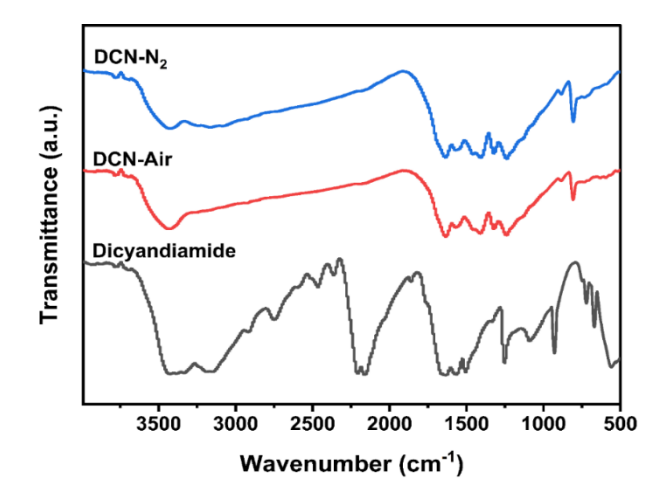


Fig. 5. FT-IR spectra of g-C₃N₄ obtained from dicyandiamide at 550°C under nitrogen and air atmosphere.

The photocatalytic properties of DCN-Air, MCN-Air, and UCN-Air synthesized under air and nitrogen atmosphere at 550°C are shown in Fig. 6. The degradation efficiency of TC for DCN-Air and MCN-Air is 27.0% and 25.6%, which is lower than that of UCN-Air (51.3%). Similarly in Fig. 6(b), UCN-N₂ sample demonstrates superior photocatalytic efficiency (59.9%) to DCN-N₂ and MCN-N₂. The comparison of degradation efficiency for different catalysts is listed in Fig. 6(c), which is consist with the results of specific surface. Larger specific surface could provide more active sites during degradation process, contributing to the enhancement of degradation efficiency. In order to analyze the reaction kinetics during TC degradation, the experimental results were fitted by the following formula [20]:

$$ln(C_0/C) = kt$$

where C_0 is the initial concentration of antibiotics, C is the concentration of antibiotics remaining in the solution after photocatalysis, k is the kinetic constant, and t is the irradiation time. As seen in Fig. 6(d), the degradation curves of all samples present a good linear relationship, suggesting that the photocatalytic degradation of all samples conforms to the first-order reaction kinetics. Specifically, the reaction constants of DCN-Air, MCN-Air, and UCN-Air for TC degradation are 0.00551, 0.00495, and 0.01192 min⁻¹, respectively. The degradation rates of DCN-N₂, MCN-N₂ and UCN-N₂ are 0.00948, 0.00806 and 0.0151 min⁻¹, respectively.

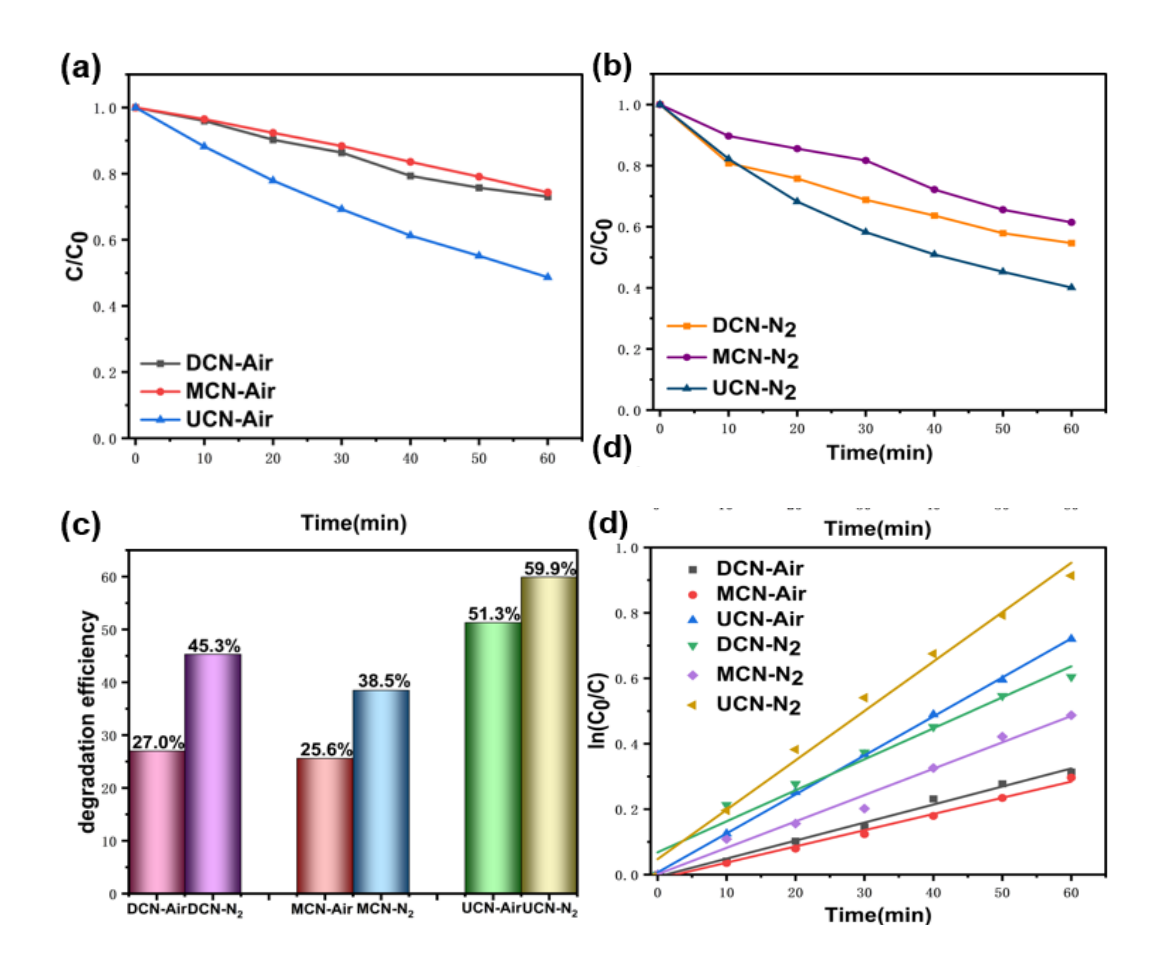


Fig. 6. Photocatalytic degradation of TC for different samples: (a) in air, (b) in nitrogen, (c) comparison of degradation efficiency, (d) corresponding first-order kinetic curves.

Fig. 7 compares the photocatalytic performance DCN samples prepared at different temperatures in air and N₂ atmosphere. It is clear that g-C₃N₄ heated at 550°C exhibits higher TC degradation efficiency both in air and N₂ atmosphere. Additionally, when the g-C₃N₄ was heated at the same temperature, the TC removal efficiency of the catalyst prepared under nitrogen atmosphere is much higher than air atmosphere. Compared to other samples, DCN-550N₂ displays a significantly improved degradation efficiency, which could be attributed to higher crystallinity as a result of synergistic effect of the nitrogen atmosphere and the optimal temperature of 550°C on the intrinsic structure of g-C₃N₄. Fig.7(d) shows the photocatalytic degradation kinetics curves of DCN samples. The reaction rate constants of DCN-450Air, DCN-550Air, and DCN-650Air, DCN-450N₂, DCN-550N₂, and DCN-650N₂ are 0.00393, 0.00551, 0.00326, 0.00678, 0.10042, and 0.00807 min⁻¹, respectively. According to the above results, DCN-550N₂ shows the highest rate constant, which is 18.2 times that of DCN-550Air sample.

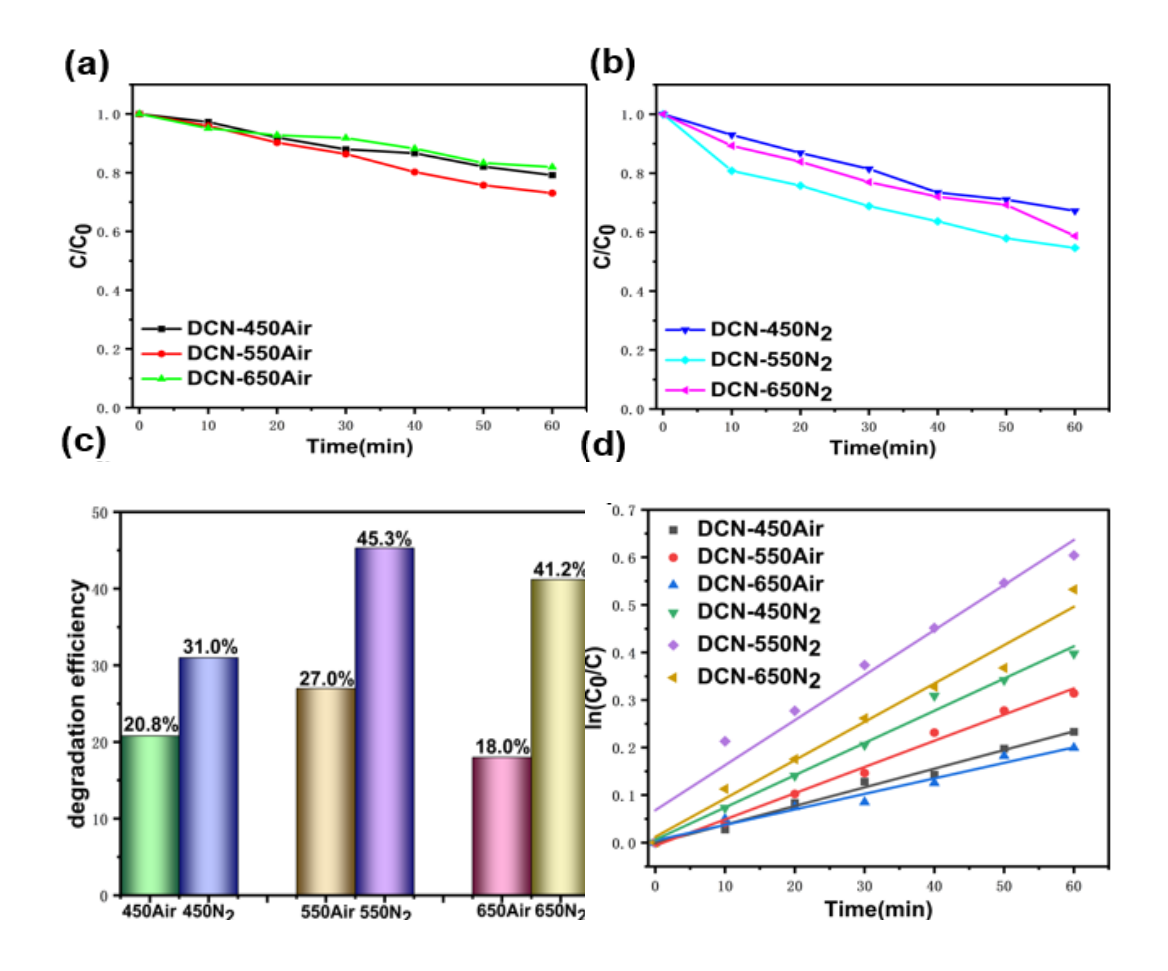


Fig. 7. TC degradation of DCN samples prepared at various temperatures: (a) in air, (b) in nitrogen, (c) comparison of degradation efficiency, (d) corresponding first-order kinetics curves.

4. Conclusion

Using dicyandiamide, melamine, and urea as precursors, g- C_3N_4 with superior photocatalytic performance was synthesized at diverse temperatures and in atmospheres. It was discovered that g- C_3N_4 prepared under nitrogen atmosphere possessed a more distinct layered structure and a smoother surface than those prepared under an air environment. At 550°C, the synthesized UCN- N_2 exhibited higher crystallinity and surface area, with the highest TC degradation efficiency of 59.9% after illumination of 60 min.

References

- [1] I. D. Godos, R. Mu[~] noz, B. Guieysse, Journal of Hazardous Materials. 229-230, 446-449(2012); https://doi.org/10.1016/j.jhazmat.2012.05.106
- [2] Q. H. Shen, L. F. Wei, R. H. Bibi, K. Wang, D. D. Hao, J. C. Zhou, N. X. Li, Journal of Hazardous Materials. 413 125376 (2021); https://doi.org/10.1016/j.jhazmat.2021.125376
- [3] D. Kılıç, M. Sevim, Z. F. Eroğlu, Ö. Metin, S. Karaca, Advanced Powder Technology.

- 32(8), 2743-2757(2021); https://doi.org/10.1016/j.apt.2021.05.043
- [4] J. J. Zhang, Y. Zhao, K. Z. Qi, S. Y. Liu, Journal of Materials Science & Technology. 172: 145-155(2024); https://doi.org/10.1016/j.jmst.2023.06.042
- [5] X. L. Chen, Y. Y. Yang, Y. C. Ke, C. Chen, S. G. Xie, Science of The Total Environment. 814 152852 (2022); https://doi.org/10.1016/j.scitotenv.2021.152852
- [6] M. Q. Luo, Z. Y. Wang, S. Fang, H. Liu, C. Zhang, P. W. Cao, D. M. Li, Chemosphere, 334, 138913 (2023); https://doi.org/10.1016/j.chemosphere.2023.138913
- [7] Q. H. Liang, X. J. liu, B. B. Shao, L. Tang, Z. F. Liu, W. Zhang, S. X. Gong, Y. Liu, Q. Y. He, T. Wu, Y. Pan, S. H. Tong, Chemical Engineering Journal. 426, 130831 (2021); https://doi.org/10.1016/j.cej.2021.130831
- [8] G. Mamba, A. K. Mishra, Applied Catalysis B: Environmental. 198, 347-377 (2016); https://doi.org/10.1016/j.apcatb.2016.05.052
- [9] K. Bisaria, S. Sinha, R. Singh, H M.N. Iqbal, Chemosphere, 284, 131263 (2021); https://doi.org/10.1016/j.chemosphere.2021.131263
- [10] Y. P. Zhu, T. Z. Ren, Z.Y. Yuan, ACS Applied. Materials & Interfaces 7(30), 16850-16856 (2015); https://doi.org/10.1021/acsami.5b04947
- [11] X. C. Wang, K. Maeda, A. Thomas, K. Takanabe, G. Xin, J M. Carlsson, K. Domen, M. Antonietti, nature materials. 8, 76-80 (2009); https://doi.org/10.1038/nmat2317
- [12] M. Razavi-Esfali, T. Mahvelati-Shamsabadi, H. Fattahimoghaddam, B.K. Lee, Chemical Engineering Journal. J. 419, 129503 (2021); https://doi.org/10.1016/j.cej.2021.129503
- [13] H. Wang, X. D. Zhang, Y. Xie, MATERIALS TODAY, 23, 72-86(2019); https://doi.org/10.1016/j.mattod.2018.05.001
- [14] A. Torres-Pinto, C. G. Silva, J L. Faria, A M.T. Silva, Catalysis Today, 424, 113868 (2023); https://doi.org/10.1016/j.cattod.2022.08.010
- [15] W. K. Darkwah, Y. H. Ao, Nanoscale Research Letters 13, 388 (2018)
- [16] G. G. Zhang, M. H. Liu, T. Heil, S. Zafeiratos, A. Savateev, M. Antonietti, X. C. Wang, Angewandte Chem International Edition. 58 (42), 14950 (2019); https://doi.org/10.1002/anie.201908322
- [17] M. F. Vega, C. Olivas, E. Díaz-Faes, C.Barriocanal, Catalysis Today, 427, 114412 (2024); https://doi.org/10.1016/j.cattod.2023.114412
- [18] Y. Q. Shao, C. C. Liu, H. R. Ma, J. J. Chen, C. L. Dong, D. J. Wang, Z. Y. Mao, Chemical Physics Letters, 801, 139748 (2022); https://doi.org/10.1016/j.cplett.2022.139748
- [19] I.Papailias, T.Giannakopoulou, N.Todorova, D. Demotikali, T.Vaimakis, C.Trapalis, Applied Surface Science, 358, 278-286 (2015); https://doi.org/10.1016/j.apsusc.2015.08.097
- [20] Q. R. Zhao, S. N. Liu, S. Y. Chen, B. H. Ren, Y. C. Zhang, X. Luo, Y. Sun, Chemical Physics Letters, 805, 139908 (2022); https://doi.org/10.1016/j.cplett.2022.139908